*Inorg. Chem.* **2007**, *46*, 1123–1134

# Iron–Molybdenum Charge-Transfer Hybrids Containing Organometallic and Inorganic Fragments Bridged by Aryldiazenido Ligands in a $\mu$-$\eta^6$:$\eta^1$ Coordination Mode: Syntheses, Characterization, X-ray Structures, Electrochemistry, and Theoretical Investigation†

**Carolina Manzur,‡ Lorena Millán,‡ Mauricio Fuentealba,‡ Jean-René Hamon,§ Loïc Toupet,|| Samia Kahlal,§ Jean-Yves Saillard,*,§ and David Carrillo*,‡**

*Laboratorio de Química Inorgánica, Instituto de Química, Pontificia Universidad Católica de Valparaíso, Avenida Brasil 2950, Valparaíso, Chile, UMR 6226 "Sciences Chimiques de Rennes", CNRS-Université de Rennes 1, Campus de Beaulieu, 35042 Rennes-Cedex, France, and UMR 6626 Groupe Matière Condensée et Matériau, CNRS-Université de Rennes 1, Campus de Beaulieu, 35042 Rennes Cedex, France*

Received July 14, 2006

Representative members of a new family of covalently bonded charge-transfer molecular hybrids, of general formula $[(\eta^5\text{-}C_5H_5)Fe(\mu,\eta^6{:}\eta^1\text{-}p\text{-}RC_6H_4NN)Mo(\eta^2\text{-}S_2CNEt_2)_3]^+PF_6^-$ (R: H, **5**$^+PF_6^-$; Me, **6**$^+PF_6^-$; MeO, **7**$^+PF_6^-$) and $[(\eta^5\text{-}C_5Me_5)Fe(\mu,\eta^6{:}\eta^1\text{-}C_6H_5NN)Mo(\eta^2\text{-}S_2CNEt_2)_3]^+PF_6^-$, **8**$^+PF_6^-$, have been synthesized by reaction of the corresponding mixed-sandwich organometallic hydrazines $[(\eta^5\text{-}C_5H_5)Fe(\eta^6\text{-}p\text{-}RC_6H_4NHNH_2)]^+PF_6^-$ (R: H, **1**$^+PF_6^-$; Me, **2**$^+PF_6^-$; MeO, **3**$^+PF_6^-$) and $[(\eta^5\text{-}C_5Me_5)Fe(\eta^6\text{-}C_6H_5NHNH_2)]^+PF_6^-$, **4**$^+PF_6^-$, with *cis*-dioxomolybdenum(VI) bis(diethyldithiocarbamato) complex, $[MoO_2(S_2CNEt_2)_2]$, in the presence of sodium diethyldithiocarbamato trihydrate, $NaSC(=S)NEt_2\cdot 3H_2O$, in refluxing methanol. These iron–molybdenum complexes consist of organometallic and inorganic fragments linked each other through a $\pi$-conjugated aryldiazenido bridge coordinated in $\eta^6$ and $\eta^1$ modes, respectively. These complexes were fully characterized by FT-IR, UV–visible, and $^1$H NMR spectroscopies and, in the case of complex **7**$^+PF_6^-$, by single-crystal X-ray diffraction analysis. Likewise, the electrochemical and solvatochromic properties were studied by cyclic voltammetry and UV–visible spectroscopy, respectively. The electronic spectra of these hybrids show an absorption band in the 462–489 and 447–470 nm regions in $CH_2Cl_2$ and DMSO, respectively, indicating the existence of a charge-transfer transition from the inorganic donor to the organometallic acceptor fragments through the aryldiazenido spacer. A rationalization of the properties of **5**$^+PF_6^-$–**8**$^+PF_6^-$ is provided through DFT calculations on a simplified model of **7**$^+PF_6^-$. Besides the heterodinuclear complexes **5**$^+PF_6^-$–**8**$^+PF_6^-$, the mononuclear molybdenum diazenido derivatives, $[(\eta^1\text{-}p\text{-}RC_6H_4NN)Mo(\eta^2\text{-}S_2CNEt_2)_3]$ (R: H, **9**; Me, **10**; MeO, **11**), resulting from the decoordination of the $[(\eta^5\text{-}C_5H_5)Fe]^+$ moiety of complexes **5**$^+PF_6^-$–**7**$^+PF_6^-$, were also isolated. For comparative studies, the crystalline and molecular structure of complex **10**$\cdot Et_2O$ was also determined by X-ray diffraction analysis and its electronic structure computed.

## Introduction

In the last four decades and since the pioneering paper of King and Bisnette describing the first (aryldiazenido)metal complex,[1] the syntheses of a considerable amount of organodiazenido compounds have been reported[2,3] and a great variety of X-ray diffraction structures has been revealed.[4] Much of the interest in transition metal complexes containing organodiazenido ligands, $R-N_\beta=N_\alpha$, arises from their potential applications as models[5] for intermediates in biological[6] and industrial[7] dinitrogen to ammonia conversion. The exceptional electronic structure of such ligands allows

* To whom correspondence should be addressed. E-mail: david.carrillo@ucv.cl (D.C.), saillard@univ-rennes1.fr (J.-Y.S.).

† This article is dedicated to our friend Professor Didier Astruc on the occasion of his 60th birthday.

‡ Pontificia Universidad Católica de Valparaíso.
§ UMR 6226, Université de Rennes 1.
|| UMR6626, Université de Rennes 1.

(1) King, R. B.; Bisnette, M. B. *J. Am. Chem. Soc.* **1964**, *86*, 5694.

10.1021/ic0613098 CCC: $37.00 
Published on Web 01/20/2007

**Scheme 1**

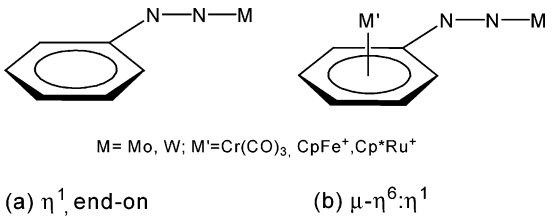


different coordination modes, and consequently, several types of geometric structures have been observed and described in the literature.[2,3] However, in the majority of mononuclear organodiazenido complexes, this ligand is bonded to transition metal centers through the terminal $N_\alpha$ atom, using its $\sigma_n$, $\pi_\sigma$, and $\pi_\pi$ frontier molecular orbitals in an $\eta^1$ or end-on coordination mode,[2,4] giving a near linear $RN_\beta{=}N_\alpha{\rightleftharpoons}M$ fragment (Scheme 1,a). In monoaryldiazenido complexes, calculations of the frontier molecular orbitals occupations suggest that the formal oxidation state of the RNN ligand is $-1$.[4] Surprisingly, novel structures, where the organodiazenido ligand acts as a spacer bridging two different metal centers through the terminal $N_\alpha$ atom and through the $\pi$-system of the aryl group in a $\eta^1$- and $\eta^6$-coordination fashions, respectively (Scheme 1b), have recently been reported by Hidai and co-workers.[8] To the best of our knowledge, this type of inorganic−organometallic hybrid is the first example reported in the literature. The complexes that contain the heterobimetallic $\{M(\mu,\eta^6{:}\eta^1\text{-}p\text{-}RC_6H_4NN)W\}$ core (M = Cr, Fe, Ru; R = H, Me, OMe, COOMe)[8,9] have been synthesized by reaction of the anionic dinitrogen complex $[W(NCS)(N_2)(dppe)_2]^-$ or the neutral diazenido complex $[WF(NNH)(dppe)_2]$ with activated $\eta^6$-fluoroarene complexes of Cr, Fe, and Ru, under mild conditions. These reactions have been suggested to proceed by a direct nucleophilic aromatic substitution mechanism.[8] These heterobinuclear complexes[9] were fully characterized by spectroscopic techniques and their molecular structures were studied by single-crystal X-ray diffraction analysis, but their charge-transfer properties were not investigated.

The versatile hapticity exhibited by the organodiazenido ligands in transition metal complexes and, particularly, the hapticity exhibited in this type of heterobinuclear complexes, the increasing interest observed on the functionalization of polyoxometalates to generate new hybrid materials[10] containing inorganic and organic or organometallic fragments linked covalently one another by an extended $\pi$-conjugated bridge, and the electronic cooperativity we have observed in CpFe(arylhydrazones) of ferrocenyl and diferrocenyl aldehydes and ketones[11] prompted our investigations toward the synthesis of new organometallic−inorganic charge-transfer hybrids. These complexes of general formula $[(\eta^5\text{-}Cp')Fe(\mu,\eta^6{:}\eta^1\text{-}p\text{-}RC_6H_4NN)Mo(\eta^2\text{-}S_2CNEt_2)_3]^+PF_6^-$, $\mathbf{5}^+PF_6^-$−$\mathbf{8}^+PF_6^-$ (Cp′ = $C_5H_5$, $C_5Me_5$), were prepared by reacting their respective organometallic hydrazine precursors $[(\eta^5\text{-}Cp')Fe(\eta^6\text{-}p\text{-}RC_6H_4NHNH_2)]^+PF_6^-$, $\mathbf{1}^+PF_6^-$−$\mathbf{4}^+PF_6^-$, with $[MoO_2(S_2CNEt_2)_2]$ in the presence of $NaSC(=S)NEt_2$. As a result, we report herein (i) the synthesis and the full characterization of a series of charge-transfer hybrids, containing the electron-withdrawing fragment $[(\eta^5\text{-}Cp')Fe]^+$ and the strong electron-releasing fragment $[Mo(\eta^2\text{-}S_2CNEt_2)_3]^+$, bridged one other by an aryldiazenido ligand, $[p\text{-}RC_6H_4NN]^-$, R = H, Me, and MeO, in a $\mu,\eta^6{:}\eta^1$ coordination mode, (ii) the crystal and molecular structure of complex $\mathbf{7}^+PF_6^-$ and the mononuclear derivative $[(\eta^1\text{-}p\text{-}MeC_6H_4NN)Mo(\eta^2\text{-}S_2CNEt_2)_3]$, $\mathbf{10}{\cdot}Et_2O$, by X-ray diffraction analysis, (iii) the effect of the nature of the Cp′ ligands on the redox properties of complexes $\mathbf{5}^+PF_6^-$ and $\mathbf{8}^+PF_6^-$ and the necessary comparison of the redox properties of complex $\mathbf{5}^+PF_6^-$ and the known compound **9**,[12]

(2) (a) Nugent, W. A.; Mayer, J. M. *Metal-Ligand Multiple Bonds*; Wiley-Interscience: New York, 1988. (b) Sutton, D. *Chem. Rev.* **1993**, *93*, 995. (c) Wigley, D. E. *Prog. Inorg. Chem.* **1994**, *42*, 239. (d) Hidai, M.; Mizobe, Y. *Chem. Rev.* **1995**, *95*, 1115. (e) Hirsch-Kuchma, M.; Nicholson, T.; Davidson, A.; Jones, A. G. *J. Chem. Soc., Dalton Trans.* **1997**, 3189. (f) Carrillo, D. *C. R. Chimie* **2000**, *3*, 175. (g) Hidai, M.; Mizobe, Y. *Can. J. Chem.* **2005**, *83*, 358.

(3) (a) Chatt, J.; Pearman, A.; Richards, R. L. *J. Chem. Soc., Dalton Trans.* **1976**, 1520. (b) Butler, G.; Chatt, J.; Leigh, G. J. *J. Chem. Soc., Chem. Commun.* **1978**, 352. (c) Leigh, G. J. *J. Organomet. Chem.* **2004**, *689*, 3999 and references therein.

(4) More than 100 papers related to structurally characterized organodiazenido transition metal complexes are gathered in the following: Kahlal, S.; Saillard, J.-Y.; Hamon, J.-R.; Manzur, C.; Carrillo, D. *New J. Chem.* **2001**, *25*, 231.

(5) Schrock, R. R. *Acc. Chem. Res.* **2005**, *38*, 955.

(6) See for example: (a) Hardy, R. W. F.; Bottomley, F.; Burns, R. C. A. *Treatise on Dinitrogen Fixation*; Wiley-Interscience: New York, 1979. (b) *Molybdenum and Molybdenum-Containing Enzymes*; Coughlan, M. P., Ed., Pergamon: New York, 1980. (c) Veeger, C.; Newton, W. E. *Advances in Nitrogen Fixation Research*; Dr. W. Junk/Martinus Nijhoff: Boston, MA, 1984. (d) Burgess, B. K.; Lowe, D. *J. Chem. Rev.* **1996**, *96*, 2983.

(7) Smil, V. *Enriching the Earth: Fritz Haber, Carl Bosch, and Transformation of World Food Production*; MIT Press: Cambridge, MA, 2004.

(8) Ishii, Y.; Kawaguchi, M.; Ishino, Y.; Aoki, T.; Hidai, M. *Organometallics* **1994**, *13*, 5062.

(9) The formulas of the heterobinuclear aryldiazenido complexes described by Hidai and co-workers[8] are the following: $[\{(CO)_3Cr(\mu\text{-}\eta^6{:}\eta^1\text{-}p\text{-}CO_2MeC_6H_4)-N{=}N\}W(NCS)(dppe)_2]{\cdot}CH_2Cl_2$; $[\{(CO)_3Cr(\mu\text{-}\eta^6{:}\eta^1\text{-}p\text{-}CO_2MeC_6H_4)-N{=}N\}WF(dppe)_2]{\cdot}2THF$; $[\{CpRu(\mu\text{-}\eta^6{:}\eta^1\text{-}C_6H_5)-N{=}N\}W(NCS)(dppe)_2]^+PF_6^-{\cdot}CH_2Cl_2$; $[\{CpFe(\mu\text{-}\eta^6{:}\eta^1\text{-}p\text{-}MeC_6H_4)-N{=}N\}WF(dppe)_2]^+PF_6{\cdot}Me_2CO$.

(10) (a) Judenstein, P. *Chem. Mater.* **1992**, *4*, 4. (b) Du, Y.; Rheingold, A. L.; Maatta, E. A. *J. Am. Chem. Soc.* **1992**, *114*, 345. (c) Strong, J. B.; Ostrander, R.; Rheingold, A. L.; Maatta, E. A. *J. Am. Chem. Soc.* **1994**, *116*, 3601. (d) Mohs, T. R.; Yap, G. P. A.; Rheingold, A. L.; Maatta, E. A. *Inorg. Chem.* **1995**, *34*, 9. (e) Hill, P. L.; Yap, G. P. A.; Rheingold, A. L.; Maatta, E. A. *J. Chem. Soc., Chem. Commun.* **1995**, 737. (f) Stark, J. L.; Young, V. G.; Maatta, E. A. *Angew. Chem., Int. Ed. Engl.* **1995**, *34*, 2547. (g) Judenstein, P.; Sanchez, C. *J. Mater. Chem.* **1996**, *6*, 511. (h) Moore, A. R.; Kwen, H.; Beatty, A. M.; Maatta, E. A. *Chem. Commun.* **2000**, 1793. (i) Strong, J. B.; Yap, G. P. A.; Ostrander, R.; Liable-Sands, L. M.; Rheingold, A. L.; Thouvenot, R.; Gouzerh, P.; Maatta, E. A. *J. Am. Chem. Soc.* **2000**, *122*, 639. (j) Wei, Y.; Xu, B.; Barnes, C. L. *J. Am. Chem. Soc.* **2001**, *123*, 4083. (k) Wei, Y.; Lu, M.; Cheung, C. F.-C.; Barnes, C. L.; Peng, Z. *Inorg. Chem.* **2001**, *40*, 5489. (l) Xu, B.; Wei, Y.; Barnes, C. L.; Peng, Z. *Angew. Chem., Int. Ed.* **2001**, *40*, 2290. (m) Lu, M.; Wei, Y.; Xu, B.; Cheung, C. F.-C.; Peng, Z.; Powell, D. R. *Angew. Chem., Int. Ed.* **2002**, *41*, 1566. (n) Xu, L.; Lu, M.; Xu, B.; Wei, Y.; Peng, Z.; Powell, D. R. *Angew. Chem., Int. Ed.* **2002**, *41*, 4129. (o) Okabe, A.; Fukushima, T.; Ariga, K.; Aida, T. *Angew. Chem., Int. Ed.* **2002**, *41*, 3414. (p) Bose, A.; He, P.; Liu, C.; Ellman, B. D.; Twieg, R. J.; Huang, S. D. *J. Am. Chem. Soc.* **2002**, *124*, 4. (q) Roesner, R. A.; McGrath, S. C.; Brockman, J. T.; Moll, J. D.; West, D. X.; Swearingen, J. K.; Castineiras, A. *Inorg. Chim. Acta* **2003**, *342*, 37. (r) Bar-Nahum, I.; Cohen, H.; Neumann, R. *Inorg. Chem.* **2003**, *42*, 3677. (s) Kang, J.; Nelson, J. A.; Lu, M.; Xie, B.; Peng, Z.; Powell, D. R. *Inorg. Chem.* **2004**, *43*, 6408. (t) Wu, P.; Li, Q.; Ge, N.; Wei, Y.; Wang, Y.; Wang, P.; Guo, H. *Eur. J. Inorg. Chem.* **2004**, 2819. (u) Lu, M.; Xie, B.; Kang, J.; Chen, F.-C.; Yang, Y.; Peng, Z. *Chem. Mater.* **2005**, *17*, 402. (v) Lu, M.; Kang, J.; Wang, D.; Peng, Z. *Inorg. Chem.* **2005**, *44*, 7711.

the precursor where the $CpFe^+$ group is absent, (iv) the effect of the solvent polarity, $CH_2Cl_2$ ($\mu = 8.90$) and DMSO ($\mu = 47.6$) on the electronic transitions of complexes $\mathbf{5}^+PF_6^-$−$\mathbf{8}^+PF_6^-$, particularly on the charge-transfer transitions, and (v) a DFT calculation which provides a rationalization of the electrochemical and spectroscopic properties and analyses the electronic communication between the metal centers in complex $\mathbf{7}^+$.

## Experimental Section

**Materials and Physical Measurements.** All manipulations were carried out under a dinitrogen atmosphere using standard Schlenk techniques and chromatographic columns with protection from light to avoid decomplexation of the $CpFe^+$ fragment. Solvents were dried by common procedures and distilled under dinitrogen before use. Reagents were purchased from commercial sources and used as received. The organometallic hydrazines $[(\eta^5\text{-Cp}')Fe(\eta^6\text{-}p\text{-}RC_6H_4\text{-}NHNH_2)]^+PF_6^-$, $\mathbf{1}^+PF_6^-$−$\mathbf{4}^+PF_6^-$ (Cp′ = $C_5H_5$,[13] $C_5Me_5$[14]), and $[MoO_2(S_2CNEt_2)_2]$[15] were synthesized according to published procedures. Solid IR spectra were recorded from KBr disks on a Perkin-Elmer, model Spectrum One, FT-IR spectrophotometer. Electronic spectra were obtained in $CH_2Cl_2$ and DMSO solutions on a Spectronic, Genesys 2, spectrophotometer. The $^1H$ and $^{13}C$ NMR spectra were recorded on a multinuclear Bruker Advance 400 Digital and Advance 500 Instruments. All NMR spectra are reported in ppm ($\delta$) relative to tetramethylsilane ($Me_4Si$), with the residual solvent proton resonance and carbon resonances used as internal standards. Coupling constants ($J$) are reported in Hertz (Hz), and integrations are reported as number of protons. High-resolution electrospray ionization mass spectra (ESI-MS) were obtained at the Centre Régional de Mesures Physiques de l'Ouest (CRMPO, Rennes, France) on a MS/MS ZabSpec TOF Micromass spectrometer (4 kV). Cyclic voltammetry experiments were performed at room temperature with a Radiometer PGZ100 potentiostat, using a standard three-electrode setup with a platinum working and platinum wire auxiliary electrodes and a Ag/AgCl electrode as the reference. Dichloromethane solutions were 1.0 mM in the compound under study and 0.1 M in the supporting electrolyte $n\text{-}Bu_4N^+\text{-}PF_6^-$ with a voltage scan rate = 0.1 V $s^{-1}$. The potentials are given against $E_{1/2}$ of the $Cp_2Fe/Cp_2Fe^+$ couple. Melting points were determined in evacuated capillaries and were not corrected. Elemental analysis were conducted on a Thermo-FINNIGAN Flash EA 1112 CHNS/O analyzer by the Microanalytical Service of the CRMPO at the University of Rennes 1 (Rennes, France).

**Synthesis of $[(\eta^5\text{-}C_5H_5)Fe(\mu,\eta^6\text{:}\eta^1\text{-}C_6H_5NN)Mo(\eta^2\text{-}S_2CNEt_2)_3]^+PF_6^-$, $\mathbf{5}^+PF_6^-$.** A solution of 100 mg (0.267 mmol) of $[(\eta^5\text{-Cp})Fe(\eta^6\text{-}C_6H_5NHNH_2)]^+PF_6^-$, $\mathbf{1}^+PF_6^-$, in dry MeOH (5 mL) was added dropwise to a Schlenk tube containing 5 mL of an orange suspension of 57.0 mg (0.134 mmol) of $[MoO_2(S_2CNEt_2)_2]$ and 30.0 mg (0.133 mmol) of $NaSC(=S)NEt_2\cdot 3H_2O$. The solution was vigorously stirred and refluxed for 5 h under dry $N_2$. It was then cooled to room temperature and concentrated under vacuum until a solid was formed. The crude solid was filtered out and then dissolved in 1.0 mL of $CH_2Cl_2$. The solution was percolated through a column containing silica gel (grade 60) suspended in hexane. First, the use of pure $Et_2O$ as eluant produced the release of a green band. Removal of the solvent under vacuum gave a green solid identified as $[(\eta^1\text{-}C_6H_5NN)Mo(\eta^2\text{-}S_2CNEt_2)_3]$, **9**, by comparison of its spectroscopic data with those of the literature.[12] A green-brownish band was then eluted with a $Et_2O/CH_2Cl_2$ (1:1) mixture. Evaporation of the solution to dryness afforded a dark solid, composed of a mixture of the green complex **9** and of the desired heterobinuclear compounds $\mathbf{5}^+PF_6^-$ (IR and $^1H$ NMR spectroscopy). In the three experiments below, this fraction was immediately discarded. Finally, elution with pure $CH_2Cl_2$ produced the release of the desired dark red band, which was collected. After the solvent was removed in vacuo, a reddish brown microcrystalline solid was isolated. Yield: 28 mg (23%). Mp: 202 °C (dec). Anal. Calcd for $C_{26}H_{40}F_6FeMoN_5PS_6$ ($M_r$ = 911.77 g $mol^{-1}$): C, 34.25; H, 4.42; N, 7.68. Found: C, 33.70; H, 3.87, N, 7.50. UV−vis [($\lambda_{max}$, nm (log $\epsilon$)] ($CH_2Cl_2$): 271 (4.63); 310 (4.47); 382 (3.87); 485 (3.76). UV−vis [($\lambda_{max}$, nm (log $\epsilon$)] (DMSO): 275 (4.57); 319 (3.56); 385 (3.83); 469 (3.82). IR (KBr, $cm^{-1}$): 3116 (vw); 3087 (vw); 3068 (w); 2977 (w); 2933 (w); 2870 (vw), $\nu$(C−H); 1511 (s), 1463 (sh); 1440 (vs), $\nu$(N═N), $\nu$(C⋯C), and/or $\nu$(C⋯N); 841 (vs), $\nu(PF_6)$; 558 (m), $\delta$(P−F). $^1H$ NMR (400 MHz, $CD_3CN$): $\delta$ 1.15 (t, 3H, $CH_2CH_3$, $J_{H-H}$ = 7.1 Hz); 1.20−1.30 (m, 15H, $CH_2CH_3$); 3.70−3.87 (m, 12H, $CH_2CH_3$); 4.80 (s, 5H, *Cp*); 5.85−5.96 (m, 3H, *Ph*); 6.06 (*pseudo* t, 2H, *Ph*).

**Synthesis of $[(\eta^5\text{-}C_5H_5)Fe(\mu,\eta^6\text{:}\eta^1\text{-}p\text{-}MeC_6H_4NN)Mo(\eta^2\text{-}S_2CNEt_2)_3]^+PF_6^-$, $\mathbf{6}^+PF_6^-$.** The procedure adopted was similar to that described for the preparation of complex $\mathbf{5}^+PF_6^-$, using in this case 133 mg (0.340 mmol) of $[(\eta^5\text{-Cp})Fe(\eta^6\text{-}p\text{-}MeC_6H_4NHNH_2)]^+PF_6^-$, $\mathbf{2}^+PF_6^-$, 73.4 mg (0.172 mmol) of $[MoO_2(S_2CNEt_2)_2]$, and 38.9 mg (0.173 mmol) of $NaSC(=S)NEt_2\cdot 3H_2O$. Workup and chromatographic separation as described above gave the green complex **10** (see below) and $\mathbf{6}^+PF_6^-$ as a reddish brown powder. Yield: 54 mg (34%). Mp: 166 °C (dec). Anal. Calcd for $C_{27}H_{42}F_6FeN_5MoPS_6$ ($M_r$ = 925.80 g $mol^{-1}$): C, 35.03; H, 4.57; N, 7.56. Found: C, 34.71; H, 4.39; N, 7.43. UV−vis [($\lambda_{max}$, nm (log $\epsilon$)] ($CH_2Cl_2$): 244 (4.57); 295 sh (3.84); 388 (3.77); 489 (3.79). UV−vis [($\lambda_{max}$, nm (log $\epsilon$)] (DMSO): 264 (4.53); 309 sh (4.07); 381 (3.77); 463 (3.73). IR (KBr, $cm^{-1}$): 3123 (vw); 3072 (vw); 2975 (w); 2930 (w); 2920 (w); 2874 (w); 2850 (w), $\nu$(C−H); 1508 (s); 1447 (sh), 1433 (vs), $\nu$(N═N), $\nu$(C⋯C) and/or $\nu$(C⋯N); 839 (vs), $\nu(PF_6)$; 558 (m), $\delta$-(P−F). $^1H$ NMR (400 MHz, $CD_3CN$): $\delta$ 1.22 (t, 3H, $CH_2CH_3$, $J_{H-H}$ = 7.1 Hz); 1.26−1.31 (m, 15H, $CH_2CH_3$); 2.16 (s, 3H, Ph−$CH_3$); 3.75−3.92 (m, 12H, $CH_2CH_3$); 4.75 (s, 5H, *Cp*); 5.85 (*pseudo* t, 1H, *Ph*); 5.97 (d, 1H, *Ph*, $J_{H-H}$ = 5.9 Hz); 6.01 (*pseudo* t, 1H, *Ph*); 6.51 (d, 1H, *Ph*, $J_{H-H}$ = 6.4 Hz).

**Synthesis of $[(\eta^5\text{-}C_5H_5)Fe(\mu,\eta^6\text{:}\eta^1\text{-}p\text{-}MeOC_6H_4NN)Mo(\eta^2\text{-}S_2CNEt_2)_3]^+PF_6^-$, $\mathbf{7}^+PF_6^-$.** This compound was prepared following a procedure similar to that described above for complex $\mathbf{5}^+PF_6^-$ using in this case 160 mg (0.396 mmol) of $[(\eta^5\text{-Cp})Fe(\eta^6\text{-}p\text{-}MeOC_6H_4NHNH_2)]^+PF_6^-$, $\mathbf{3}^+PF_6^-$, 84.0 mg (0.198 mmol) of


(11) (a) Manzur, C.; Millán, L.; Fuentealba, M.; Hamon, J.-R.; Carrillo, D. *Tetrahedron Lett.* **2000**, *41*, 361. (b) Manzur, C.; Fuentealba, M.; Carrillo, D.; Boys, D.; Hamon, J.-R. *Bol. Soc. Chil. Quim.* **2001**, *46*, 409. (c) Manzur, C.; Fuentealba, M.; Millán, L.; Gajardo, F.; Carrillo, D.; Mata, J. A.; Sinbandhit, S.; Hamon, P.; Hamon, J.-R.; Kahlal, S.; Saillard, J.-Y. *New J. Chem.* **2002**, *26*, 213. (d) Manzur, C.; Fuentealba, M.; Millán, L.; Gajardo, F.; Garland, M. T.; Baggio, R.; Mata, J. A.; Hamon, J.-R.; Carrillo, D. *J. Organomet. Chem.* **2002**, *660*, 71. (e) Trujillo, A.; Fuentealba, M.; Manzur, C.; Carrillo, D.; Hamon, J.-R. *J. Organomet. Chem.* **2003**, *681*, 150. (f) Manzur, C.; Zúñiga, C.; Millán, L.; Fuentealba, M.; Mata, J. A.; Hamon, J.-R.; Carrillo, D. *New J. Chem.* **2004**, *28*, 134. (g) Manzur, C.; Millán, L.; Fuentealba, M.; Mata, J. A.; Carrillo, D.; Hamon, J.-R. *J. Organomet. Chem.* **2005**, *690*, 1265. (h) Figueroa, W.; Fuentealba, M.; Manzur, C.; Vega, A. I.; Carrillo, D.; Hamon, J.-R. *C. R. Chimie* **2005**, *8*, 1268.

(12) Dilworth, J. R.; Neaves, B. D.; Pickett, C. J. *Inorg. Chem.* **1980**, *19*, 2859.

(13) (a) Neto, A. F.; Miller, J. *An. Acad. Bras. Cienc.* **1982**, *54*, 331. (b) Piórko, A.; Sutherland, R. G.; Vessières-Jaouen, A.; Jaouen, G. *J. Organomet. Chem.* **1996**, *512*, 79. (c) Manzur, C.; Baeza, E.; Millán, L.; Fuentealba, M.; Hamon, P.; Hamon, J.-R.; Boys, D.; Carrillo, D. *J. Organomet. Chem.* **2000**, *608*, 126.

(14) Fuentealba, M.; Toupet, L.; Manzur, C.; Carrillo, D.; Hamon, J.-R. *J. Organomet. Chem.* **2006**, doi:10.1016/j.jorganchem.2006.11.008.

(15) Moore, F. W.; Larson, M. L. *Inorg. Chem.* **1967**, *6*, 998.

**Table 1.** Crystallographic Data Collection and Structure Refinement Parameters for Complexes $\mathbf{7}^{+}PF_6^{-}$ and $\mathbf{10}\cdot OEt_2$

| param | $\mathbf{7}^{+}PF_6^{-}$ | $\mathbf{10}\cdot OEt_2$ |
|---|---|---|
| empirical formula | $C_{27}H_{42}F_6FeMoN_5OPS_6$ | $C_{26}H_{47}MoN_5OS_6$ |
| formula mass, g mol$^{-1}$ | 941.77 | 733.99 |
| collcn *T*, K | 120(1) | 130(1) |
| cryst system | triclinic | triclinic |
| space group | *P*$\bar{1}$ | *P*$\bar{1}$ |
| *a* (Å) | *10.0854(3)* | *10.5071(7)* |
| *b* (Å) | *16.2396(7)* | *13.0548(7)* |
| c (Å) | 25.2360(9) | 13.1799(9) |
| α (deg) | 92.994(3) | 85.927(5) |
| *β* (deg) | 93.952(3) | 85.955(4) |
| *γ* (deg) | 107.908(3) | 75.668(4) |
| *V* (Å$^3$) | *3911.9(2)* | *1744.55(19)* |
| *Z* | 4 | 2 |
| $D_{calcd}$ (g cm$^{-3}$) | 1.599 | 1.397 |
| cryst size (mm) | 0.22 × 0.18 × 0.08 | 0.12 × 0.12 × 0.03 |
| *F*(000) | 1920 | 768 |
| abs coeff (mm$^{-1}$) | 1.111 | 0.762 |
| *θ* range (deg) | 2.35−27.53 | 3.10−27.26 |
| range *h*, *k*, *l* | 0/13, −21/20, −32/32 | 0/13, −15/16, −16/16 |
| no. of indepdt reflcns | 17 367 | 7688 |
| no. unique reflcns (>2*σ*) | 10 662 | 5197 |
| data/restraints/params | 17 367/0/865 | 7688/0/353 |
| final R indices [$I > 2\sigma(I)$] | $R_1 = 0.0776$; $wR_2 = 0.1578$ | $R_1 = 0.0555$; $wR_2 = 0.1069$ |
| R indices (all data) | $R_1 = 0.1732$; $wR_2 = 0.1942$ | $R_1 = 0.1015$; $wR_2 = 0.1266$ |
| goodness of fit/$F^2$ | 1.119 | 1.033 |
| largest diff peak and hole (e·A$^{-3}$) | 1.051 and −0.672 | 0.844 and −0.613 |

$[MoO_2(S_2CNEt_2)_2]$, and 44.0 mg (0.195 mmol) of $NaSC(=S)NEt_2\cdot 3H_2O$. The solution was refluxed for 1 h. Workup and chromatographic separation as described above gave the green complex **11** (see below) and $\mathbf{7}^{+}PF_6^{-}$ as a reddish brown powder. Single crystals of $\mathbf{7}^{+}PF_6^{-}$ suitable for X-ray diffraction studies were obtained by slow diffusion of diethyl ether into a concentrated dichloromethane solution, at room temperature. Yield: 60 mg (33%). Mp: 169 °C (dec). Anal. Calcd for $C_{27}H_{42}F_6FeMoN_5OPS_6$ ($M_r$ = 941.80 g mol$^{-1}$): C, 34.43; H, 4.49; N, 7.44. Found: C, 34.22; H, 4.40; N, 7.36. UV−vis [$\lambda_{max}$, nm (log $\epsilon$)] ($CH_2Cl_2$): 256 (4.56); 304 sh (4.11); 365 (3.80); 478 (3.71). UV−vis [($\lambda_{max}$, nm (log $\epsilon$)] (DMSO): 274 (4.57); 305 sh (3.11); 382 (3.74); 470 (3.83). IR (KBr, cm$^{-1}$): 2964 (w); 2920 (w); 2870 (w); 2853(w), *ν*(C−H); 1506 (s); 1436 (vs), *ν*(N═N), *ν*(C⋯C) and/or *ν*(C⋯N); 1256 (m), *ν*(C−O); 840 (vs), *ν*($PF_6$); 558 (m), *δ*(P−F). $^1$H NMR (400 MHz, $CD_3CN$): *δ* 1.22 (t, 3H, $CH_2CH_3$, $J_{H-H}$ = 7.1 Hz); 1.26−1.32 (m, 15H, $CH_2CH_3$); 3.76−3.86 (m, 12H, $CH_2CH_3$); 3.88 (s, 3H, $OCH_3$); 4.83 (s, 5H, *Cp*); 5.88 (d, 2H, *Ph*, $J_{H-H}$ = 6.9 Hz); 5.98 (d, 2H, *Ph*, $J_{H-H}$ = 6.9 Hz).

**Synthesis of $[(\eta^5\text{-}C_5Me_5)Fe(\mu,\eta^6\text{:}\eta^1\text{-}C_6H_5NN)Mo(\eta^2\text{-}S_2CNEt_2)_3]^{+}PF_6^{-}$, $\mathbf{8}^{+}PF_6^{-}$.** This compound was synthesized following a procedure similar to that described above for complex $\mathbf{5}^{+}PF_6^{-}$, using in this case 100 mg (0.225 mmol) of $[(\eta^5\text{-}C_5Me_5)Fe(\eta^6\text{-}C_6H_5NHNH_2)]^{+}PF_6^{-}$, $\mathbf{4}^{+}PF_6^{-}$, 48.0 mg (0.113 mmol) of $[MoO_2(S_2CNEt_2)_2]$, and 28.0 mg (0.124 mmol) of $NaSC(=S)NEt_2\cdot 3H_2O$. Workup and chromatographic separation as described above for the Cp counterparts gave the green complex **9**[12] and $\mathbf{8}^{+}PF_6^{-}$ as a reddish brown powder. Yield: 91 mg (82%). Mp: 200 °C. Anal. Calcd for $C_{31}H_{50}F_6FeMoN_5PS_6$ ($M_r$ = 981.91 g mol$^{-1}$): C, 37.92; H, 5.13; N, 7.13. Found: C, 37.44; H, 5.22; N, 6.83%. UV−vis [$\lambda_{max}$, nm (log $\epsilon$)] ($CH_2Cl_2$): 261 (4.71); 321 sh (4.02); 382 (3.78); 462 (3.90). UV−vis [($\lambda_{max}$, nm (log $\epsilon$)] (DMSO): 257 (4.53); 294 sh (4.41); 386 (3.53); 447 (3.92). IR (KBr, cm$^{-1}$): 3073 (vw); 2978 (w); 2920 (w); 2870 (vw), 2850 (vw), *ν*(C−H); 1512 (s); 1500 (s), 1445 (vs); 1436 (vs), *ν*(N═N), *ν*(C⋯C) and/or *ν*(C⋯N); 839 (vs), *ν*($PF_6$); 558 (s), *δ*(P−F). $^1$H NMR (400 MHz, $CD_3CN$): *δ* 1.20 (t, 3H, $CH_2CH_3$, $J_{H-H}$ = 7.1 Hz); 1.22−1.38 (m, 15H, $CH_2CH_3$); 1.83 (s, 15H, $C_5-CH_3$); 3.72−3.90 (m, 12H, $CH_2CH_3$); 5.42 (d, 2H, *Ph*, $J_{H-H}$ = 6.4 Hz); 5.52 (t, 1H, *Ph*, $J_{H-H}$ = 5.9 Hz); 5.62 (t, 2H, *Ph*, $J_{H-H}$ = 6.4 Hz).

**Characterization of $[(\eta^1\text{-}p\text{-}MeC_6H_4NN)Mo(\eta^2\text{-}S_2CNEt_2)_3]\cdot Et_2O$, $\mathbf{10}\cdot Et_2O$.** Crystals of $\mathbf{10}\cdot Et_2O$ suitable for X-ray structure determination were grown by slow evaporation of a concentrated diethyl ether solution at room temperature. Mp: 158 °C. Anal. Calcd for $C_{26}H_{47}MoON_5S_6$ ($M_r$ = 734.02 g mol$^{-1}$): C, 42.54; H, 6.45; N, 9.54. Found: C, 42.36; H, 6.36; N, 9.44. UV−vis [$\lambda_{max}$, nm (log $\epsilon$)] ($CH_2Cl_2$): 253 (4.57); 305 sh (4.08); 412 (3.98); 537 (2.78). UV−vis [($\lambda_{max}$, nm (log $\epsilon$)] (DMSO): 247 (4.55); 304 sh (3.99); 414 (3.90); 512 (2.77). IR (KBr, cm$^{-1}$): 2972 (w); 2928 (w); 2845 (vw); 2868 (vw), *ν*(C−H); 1532 (m); 1532 (s), 1505(s), 1487 (s), 1454 (m), 1430(s), *ν*(N═N) and *ν*(C⋯C) and/or *ν*(C⋯N). $^1$H NMR (500 MHz, $CD_3COCD_3$): *δ* 1.13 (t, 6H, $O-CH_2-CH_3$, $J_{H-H}$ = 7.0 Hz); 1.22 (t, 3H, $N-CH_2-CH_3$, $J_{H-H}$ = 6.8 Hz); 1.30 (*pseudo* q, 15H, $N-CH_2-CH_3$); 2.35 (br s, 3H, $p\text{-}CH_3C_6H_4$); 3.44 (q, 4H, $O-CH_2-CH_3$, $J_{H-H}$ = 7.0 Hz); 3.81−3.87 (m, 12H, $N-CH_2-CH_3$); 7.02 (br s, 4H, $C_6H_4$). $^{13}$C NMR (125 MHz, $CD_3COCD_3$): 11.56, 11.94 (2 × $1CH_3$, $NEt_2$); 11.85, 12.09 (2 × $2CH_3$, $NEt_2$); 14.76 ($CH_3$, $OEt_2$); 19.91 ($p\text{-}CH_3C_6H_4$); 43.38, 43.57 (2 × $2CH_2$, $NEt_2$); 44.90, 45.50 (2 × $1CH_2$, $NEt_2$); 65.26 ($CH_2$, $OEt_2$); 120.4 ($N-o\text{-}C_6H_4$); 121.9 ($Me-C_{ipso}$); 129.0 ($N-m\text{-}C_6H_4$); 132.9 ($N-C_{ipso}$); 199.14 ($S_2CNEt_2$). HRMS (positive ESI, methanol, $[M-H]^+$, *m*/*z*): calcd for $C_{22}H_{38}{}^{98}MoN_5S_6$, 662.0506; found, 662.0480.

**Characterization of $[(\eta^1\text{-}p\text{-}MeOC_6H_4NN)Mo(\eta^2\text{-}S_2CNEt_2)_3]$, 11**. Only minute amounts of pure green powdered complex **11** were isolated as a side product of the preparation of $\mathbf{7}^{+}PF_6^{-}$ (see above). Mp: 186 °C. IR (KBr, cm$^{-1}$): 2972 (w); 2928 (w); 2862 (vw), *ν*(C−H); 1538 (sh); 1498 (sh), 1490 (vs), 1459 (m), 1431 (s), *ν*(N═N) or *ν*(C⋯N); 1268 (s), *ν*(C−O). HRMS (positive ESI, methylene chloride, $[M]^+$, *m*/*z*): calcd for $C_{22}H_{37}{}^{98}MoN_5OS_6$, 677.0373; found, 677.0370.

**Crystallographic Data Collection and Structure Determinations for $\mathbf{7}^{+}PF_6^{-}$ and $\mathbf{10}\cdot Et_2O$.** Suitable crystals of complexes $\mathbf{7}^{+}PF_6^{-}$ and $\mathbf{10}\cdot Et_2O$ for data collection were selected and mounted with epoxy cement on the tip of a glass fiber. Crystal data collection and refinement parameters are given in Table 1. Compounds $\mathbf{7}^{+}PF_6^{-}$ and $\mathbf{10}\cdot Et_2O$ were studied on a Kappa-CCD Enraf-Nonius diffrac-

tometer equipped with a bidimensional CCD detector employing graphite-monochromated Mo Kα radiation ($\lambda = 0.710\ 73$ Å). The cell parameters were obtained with Denzo and Scalepack with 10 frames ($\psi$ rotation: 1°/frame).[16] The data collection[17] ($2\theta_{max} = 54°$, 1491 frames via 0.3° $\omega$ rotation and 30 s/frame; $2\theta_{max} = 54°$, 160 frames via 2.0° $\omega$ rotation and 300 s/frame) provided reflections for $\mathbf{7}^{+}PF_6^{-}$ and $\mathbf{10}\cdot Et_2O$, respectively. Subsequent data reduction with Denso and Scalepack[16] gave the independent reflections (Table 1). The two structures were solved with SIR 97 which revealed the non-hydrogen atoms.[18] After anisotropic refinement, the remaining atoms were found in Fourier difference maps. The complete structures were then refined with SHELX97 by full-matrix least-squares procedures on reflection intensities ($F^2$).[19] The absorption was not corrected. In both cases the non-hydrogen atoms were refined with anisotropic displacement coefficients, and all hydrogen atoms were treated as idealized contributions. There are two chemically equivalent but crystallographically independent molecules in the asymmetric unit of $7^{+}PF_6^{-}$. The relatively high *R* value for $7^{+}PF_6^{-}$ is due to a rather large mosaicity (1.63°). Atomic scattering factors were taken from the literature.[20] ORTEP views of $\mathbf{7}^{+}PF_6^{-}$ and $\mathbf{10}\cdot Et_2O$ were generated with ORTEP3 for Windows.[21] Compounds $\mathbf{7}^{+}PF_6^{-}$ and $\mathbf{10}\cdot Et_2O$ are CCDC reference nos. 253301 and 261935, respectively. See http://www.ccdc.cam.ac.uk.

**Computational Details.** Density functional theory (DFT) calculations were carried out on the model compounds $\mathbf{7'}^{2+/+/0}$ and $\mathbf{10'}^{+/0/-}$ using the Amsterdam Density Functional (ADF) program,[22] developed by Baerends and co-workers.[23] Electron correlation was treated within the local density approximation (LDA) in the Vosko−Wilk−Nusair parametrization.[24] The nonlocal corrections of Becke and Perdew were added to the exchange and correlation energies, respectively.[25,26] The numerical integration procedure applied for the calculations was developed by te Velde et al.[23e] Spin-unrestricted calculations were carried out on all the odd-electrons systems. The atom electronic configurations were described by a triple-ζ Slater-type orbital (STO) basis set for H 1s, C 2s and 2p, N 2s and 2p, O 2s and 2p, and S 3s and 3p augmented with a 3d single-ζ polarization for C, N, O, and S atoms and with a 2p single-ζ polarization for H atoms. A triple-ζ STO basis set was used for Fe 3d and 4s and for Mo 4d and 5s augmented with a single-ζ 4p polarization function for Fe and a single-ζ 5p polarization function

**Scheme 2**

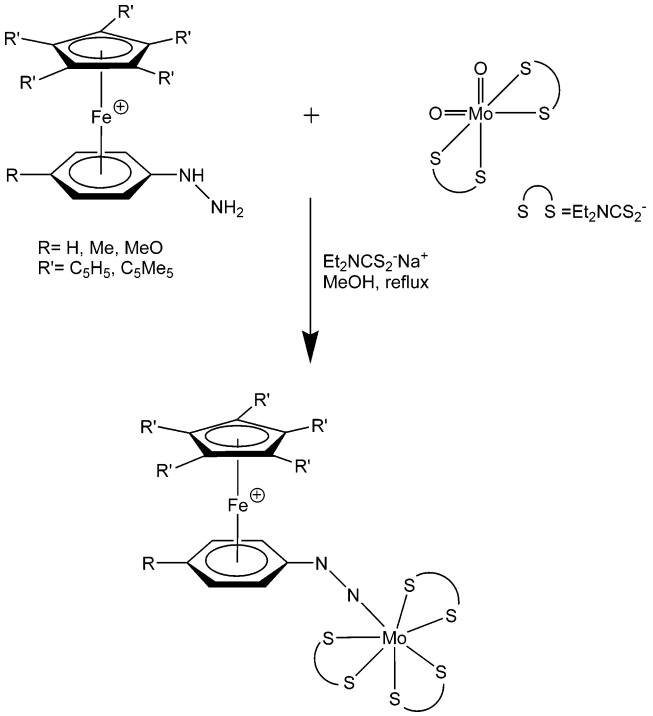


Mo. A frozen-core approximation was used to treat the core shells up to 1s for C, N, and O, 2p for S, 3p for Fe, and 4p for Mo atoms.[23] Full geometry optimizations were carried out using the analytical gradient method implemented by Verluis and Ziegler.[27] The LB94 potential,[28] which provides a correct Coulombic asymptotic behavior in the inner atomic region, was used for the TD-DFT excited-state calculations (atomic basis set unchanged). The Kohn−Sham MOs were obtained using the LB94 method. The excitation energies and oscillator strengths were calculated by following the procedure described by van Gisbergen and co-workers.[29] Representation of the orbitals were done using MOLEKEL4.3.[30]

## Results and Discussion

**Syntheses.** As shown in Scheme 2, the heterodimetallic organodiazenido complexes $\mathbf{5}^{+}PF_6^{-}$−$\mathbf{7}^{+}PF_6^{-}$ were prepared in 23−34% yield, while complex $\mathbf{8}^{+}PF_6^{-}$, which contains the $C_5Me_5^{-}$ ligand, was isolated in 82% yield, by reaction of organometallic hydrazines $\mathbf{1}^{+}PF_6^{-}$−$\mathbf{4}^{+}PF_6^{-}$, respectively, with $[MoO_2(S_2CNEt_2)_2]$ in the presence of sodium diethyldithiocarbamato trihydrate, $NaSC(=S)NEt_2\cdot 3H_2O$ (2:1:1), in refluxing methanol. This synthetic strategy is analogous to that reported for classic organodiazenido derivatives [($\eta^1$-ArNN)Mo($\eta^2$-$S_2CNR_2$)$_3$] (R= alkyl, aryl).[31,32] The known complex **9**,[12] and the two new mononuclear diazenido molybdenum compounds [($\eta^1$-*p*-$MeC_6H_4NN$)Mo($\eta^2$-$S_2$-$CNEt_2$)$_3$], **10**, and [($\eta^1$-*p*-$MeOC_6H_4NN$)Mo($\eta^2$-$S_2CNEt_2$)$_3$], **11**, were also isolated as green microcrystalline powder after chromatographic workup.


(16) Otwinowski, Z.; Minor, W. Processing of X-ray Diffraction Data Collected In Oscillation Mode. In *Methods in Enzymology, Vol. 276, Macromolecular Crystallography*; Carter, C. W., Sweet, R. M. Eds.; Academic Press: London, 1997; Part A, p 307.
(17) *Nonius Kappa CCD Software*; Nonius BV: Delft, The Netherlands, 1999.
(18) Altomare, A.; Burla, M. C.; Camalli, M.; Cascarano, G. L.; Giacovazzo, C.; Guagliardi, A.; Moliterni, A. G. G.; Polidori, G.; Spagna, R. *J. Appl. Crystallogr.* **1999**, *32*, 115.
(19) Sheldrick, G. M. *SHELX97. Program for the Refinement of Crystal Structures*; University of Göttingen: Göttingen, Germany, 1997.
(20) *International Tables for X-ray Crystallography*; Wilson, A. J. C., Ed.; Kluwer Academic Publishers: Dordrecht, The Netherlands, 1992; Vol. C.
(21) Farrugia, L. J. *J. Appl. Crystallogr.* **1997**, *30*, 565.
(22) *ADF2002.01, Theoretical Chemistry*; Vrije Universiteit: Amsterdam, The Netherlands, 2002.
(23) (a) Baerends, E. J.; Ellis, D. E.; Ros, P. *Chem. Phys.* **1973**, *2*, 41. (b) te Velde, G.; Baerends, E. J. *J. Comput. Phys.* **1992**, *99*, 84. (c) Fonseca Guerra, C.; Snijders, J. G.; te Velde, G.; Baerends, E. J. *Theor. Chem. Acc.* **1998**, *99*, 391. (d) Bickelhaupt, F. M.; Baerends, E. J. *Rev. Comput. Chem.* **2000**, *15*, 1. (e) te Velde, G.; Bickelhaupt, F. M.; Fonseca Guerra, C.; van Gisbergen, S. J. A.; Baerends, E. J.; Snijders, J. G.; Ziegler, T. *J. Comput. Chem.* **2001**, *22*, 931.
(24) Vosko, S. D.; Wilk, L.; Nusair, M. *Can. J. Chem.* **1990**, *58*, 1200.
(25) (a) Becke, A. D. *J. Chem. Phys.* **1986**, *84*, 4524. (b) Becke, A. D. *Phys. Rev. A* **1988**, *38*, 3098.
(26) (a) Perdew, J. P. *Phys. Rev. B* **1986**, *33*, 8822. (b) Perdew, J. P. *Phys. Rev. B* **1986**, *34*, 7406.
(27) Verluis, L.; Ziegler, T. *J. Chem. Phys.* **1988**, *88*, 322.
(28) van Leeuwen, R.; Baerends, E. J. *Phys. Rev. A* **1994**, *49*, 2421.
(29) van Gisbergen, S. J. A.; Snijders, J. G.; Baerends, E. J. *Comput. Phys. Commun.* **1999**, *118*, 119.
(30) Flükiger, P.; Lüthi, H. P.; Portmann, S.; Weber, J. Swiss Center for Scientific Computing (CSCS), Switzerland, 2000−2002.
(31) Bishop, M. W.; Butler, G.; Chatt, J.; Dilworth, J. R.; Leigh, G. J. *J. Chem. Soc., Dalton Trans.* **1979**, 1843.
(32) Dilworth, J. R.; Miller, J. R. *J. Chem. Educ.* **1991**, *68*, 788.

The low yields obtained for the cyclopentadienyl derivatives $\mathbf{5}^{+}PF_6^{-}-\mathbf{7}^{+}PF_6^{-}$ are presumably due to partial decoordination of the $CpFe^{+}$ moiety at an early stage of the reaction. In contrast, the bulky and electron-releasing $C_5Me_5$ ligand should play an important role in stabilizing a common key intermediate, thus leading to the isolation of $\mathbf{8}^{+}PF_6^{-}$ in high yield. Once formed, compounds $\mathbf{5}^{+}PF_6^{-}-\mathbf{7}^{+}PF_6^{-}$ are thermally stable (mp > 165 °C). They are light sensitive in solution, while, as expected, the pentamethyl analogue $\mathbf{8}^{+}PF_6^{-}$ is stable under the same conditions.[33] However, complexes $\mathbf{5}^{+}PF_6^{-}-\mathbf{7}^{+}PF_6^{-}$ can be stored as solids in the dark for several months. Despite the fact that the bimetallic complexes $\mathbf{5}^{+}PF_6^{-}-\mathbf{8}^{+}PF_6^{-}$ are ionic and the mononuclear species **9**−**11** are neutral, they cannot be cleanly separated by dissolution/precipitation sequences. This also renders their chromatographic separation difficult (see Experimental Section) and, consequently, reduces the yields of the heterobinuclear complexes.

These iron−molybdenum complexes were isolated as reddish brown microcrystalline diamagnetic solids, soluble in $CH_2Cl_2$, $Me_2CO$, MeCN, and DMSO, slightly soluble in MeOH, and insoluble in hexane. Complexes $\mathbf{5}^{+}PF_6^{-}-\mathbf{8}^{+}PF_6^{-}$, **10**, and **11** were fully characterized by FT-IR, UV−visible, and $^1$H NMR spectroscopies and elemental analysis; complex **10**·$Et_2O$ was also characterized by $^{13}$C NMR spectroscopy and high-resolution electro spray ionization mass spectrometry (ESI-MS). Some analytical data exhibit some minor deviations which are presumably due to the presence of minute amounts of solvated diethyl ether (beyond the accuracy of the NMR detection) that could not be removed by vacuum drying. However, they are consistent with the proposed structures. Complexes $\mathbf{5}^{+}PF_6^{-}-\mathbf{8}^{+}PF_6^{-}$ consist of organometallic and inorganic fragments bridged by an aryldiazenido ligand in a $\mu,\eta^6{:}\eta^1$ fashion, the molybdenum center adopting a pentagonal bipyramidal geometry. On the other hand, the crystal and molecular structures of complexes $\mathbf{7}^{+}PF_6^{-}$ and **10**·$Et_2O$ were solved by single-crystal X-ray diffraction analysis (vide infra).

The classic reaction of monosubstituted hydrazines with transition metal coordination compounds containing *cis*-(O═M═O) moieties, M = Mo, W, and Re coordinated by different types of ancillary ligands, has demonstrated to be an effective one-pot experimental procedure for the synthesis of a great variety of mono- and *cis*-bis(organodiazenido) complexes.[34] Nevertheless, the mechanisms of this well-known reaction is far from being well understood at present or, at least, remains unclear. However, it seems admissible to take into account, although from a speculative point of view, that the reaction may be viewed formally as a simple condensation reaction of the *cis*-$MoO_2$ group with the organohydrazine, $RNHNH_2$, R = alkyl and aryl, to afford $H_2O$ and the probable O═Mo═N−NHR intermediate. The removal of the remaining NH hydrogen atom can be carried out through the formation of the HO−Mo species involving some internal redox step.[35] A further substitution of the hydroxyl group in this intermediate by the free dithiocarbamate ligand, present in the reaction mixture, could lead to the formation of the heptacoordinate molybdenum complex. The presence of $NaSC(=S)NEt_2$ is an important factor to increase the yield of this class of coordination compounds.

**Spectroscopy and Electrochemistry.** The most remarkable features observed in the IR spectra of complexes $\mathbf{5}^{+}PF_6^{-}-\mathbf{7}^{+}PF_6^{-}$ is the presence of (i) two characteristic and prominent absorption bands in the 1506−1511 and 1433−1463 $cm^{-1}$ regions, attributed to the $\nu$(N═N) mode of the aryldiazenido or the $\nu$(C···N) mode of the diethyldithiocarbamato ligands,[31,32] and (ii) two typical bands, one, very strong, in the 839−841 $cm^{-1}$ region and the other one, of medium intensity, at 558 $cm^{-1}$, which correspond to the $\nu$-($PF_6$) and $\delta$(P−F) modes,[10] respectively. The spectrum of complex $\mathbf{8}^{+}PF_6^{-}$ is quite similar to those of complexes $\mathbf{5}^{+}PF_6^{-}-\mathbf{7}^{+}PF_6^{-}$, except the band attributed to the $\nu$(N═N) mode which splits yielding two identical strong and sharp bands at 1512 and 1500 $cm^{-1}$. On the other hand, the neutral molybdenum complex **10**·$Et_2O$ and **11** display a characteristic pattern in the 1550−1400 $cm^{-1}$ range, quite similar to that showed for the reported complexes $[(\eta^1\text{-}C_6H_5NN)Mo(\eta^2\text{-}S_2CNMe_2)_3]$.[32]

The UV−visible spectral data for the iron−molybdenum complexes $\mathbf{5}^{+}PF_6^{-}-\mathbf{8}^{+}PF_6^{-}$ have been recorded in $CH_2Cl_2$ and DMSO (see Experimental Section). The four complexes exhibit similar spectra, indicating similar structural features. They exhibit two overlapped absorption bands attributed to intraligand charge-transfer excitations placed, the more intense band, in the 244−271 nm range and the other one, much less intense, in the 295−321 nm range. Additionally, two less intense visible bands are observed in the 350−700 nm region: (i) a band at 382−386 nm which is not solvent-dependent and (ii) a lower energy band in the 462−489 nm region attributed to a $Mo^{IV} \rightarrow Fe^{II}$ charge-transfer excitation through the aryldiazenido spacer, which exhibits a negative solvatochromism[36] by 8−26 nm with increasing solvent polarity, i.e., on moving from $CH_2Cl_2$ ($\mu$ = 8.90) to DMSO ($\mu$ = 47.6) (Figure 1). This indicates a change in the dipole moment upon excitation from a more charge-localized ground state, with a high dipole moment, to an excited state where the positive charge is more delocalized throughout the entire molecule and the dipole moment is lower.[37] This band assignment has been supported by our TD-DFT calculations (vide infra).

The $^1$H NMR spectra of complexes $\mathbf{5}^{+}PF_6^{-}-\mathbf{8}^{+}PF_6^{-}$ are consistent with the proposed formulas. The sandwich moiety $[CpFe(\eta^6\text{-}p\text{-}RC_6H_4-)]^{+}$ is clearly identified by a single resonance at ca. 4.8 ppm attributable to the Cp moiety and two to four resolved signals of cumulative relative intensity

(33) Hamon, J.-R.; Astruc, D.; Michaud, P. *J. Am. Chem. Soc.* **1981**, *103*, 758.

(34) Gouzerh, P.; Proust, A. *Chem. Rev.* **1998**, *98*, 77 and references therein.

(35) (a) Hsieh, T.-C.; Zubieta, J. A. *Polyhedron* **1986**, *5*, 305. (b) Hsieh, T.-C.; Shaikh, S. N.; Zubieta, J. *Inorg. Chem.* **1987**, *26*, 4079.

(36) (a) Lever, A. B. P. *Inorganic Electronic Spectroscopy*, 2nd ed.; Elsevier: Amsterdam, 1984; pp 208−212. (b) Reichardt, C. *Chem. Rev.* **1994**, *94*, 2319.

(37) Dodsworth, E. S.; Hasegawa, M.; Bridge, M.; Linert, W. Fundamentals: Physical Methods, Theoretical Analysis, and Case Studies. In *Comprehensive Coordination Chemistry II; From Biology to Nanotechnology*; Lever, A. B. P., Ed.; Elsevier: New York, 2003; Vol. 2, pp 351−365.

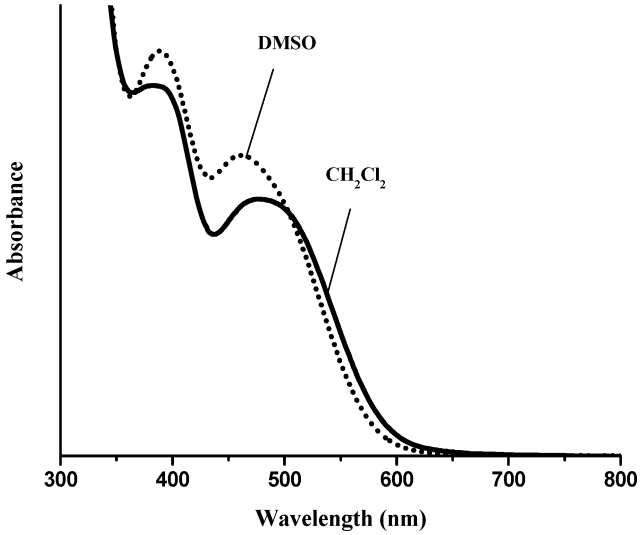


**Figure 1.** Visible bands in the electronic spectrum of complex $\mathbf{5}^+PF_6^-$.

5H ($\mathbf{5}^+$) or 4H ($\mathbf{6}^+$, $\mathbf{7}^+$, and $\mathbf{8}^+$) that correspond to the upfield $\pi$-coordinated aromatic protons. Singlet resonances were also observed at $\delta = 2.16$ (*p*-Me) and 3.88 (*p*-MeO), for $\mathbf{6}^+$ and $\mathbf{7}^+$, respectively, whereas the $C_5Me_5$ ligand of compound $\mathbf{8}^+$ exhibited its characteristic sharp peak integrating for 15 protons at $\delta = 1.83$ ppm. In addition, for the four bimetallic compounds, the $[Mo(\eta^2\text{-}S_2CNEt_2)_3]^+$ fragment gave rise to a triplet at ca. 1.20 ppm and a multiplet centered at ca. 1.25−1.30 ppm, attributable to the methyl protons of the $NEt_2$ groups, and a second multiplet at ca. 3.85 ppm assigned to the methylene protons of the $NEt_2$ groups, with the 3:15:12 relative intensity. $^1$H NMR spectrum of crystals of $\mathbf{10}\cdot Et_2O$, from which a well-shaped one was selected for the X-ray analysis (vide infra), clearly showed the presence of both the neutral molybdenum complex and the solvated diethyl ether in the ratio 1:1. Accordingly, the triplet and quartet attributed to the solvate molecule were seen at 1.13 and 3.44 ppm, respectively, while the signal pattern of **10** is quite similar to that of $\mathbf{6}^+$ with the exception of the Cp resonance and the downfield shift of the aromatic protons to 7.02 ppm. With the aid of 2-D homo- and heteronuclear NMR spectroscopy it was possible to distinguish signals corresponding to four types of ethyl groups in the room-temperature $^{13}$C NMR spectrum of $\mathbf{10}\cdot Et_2O$. This is in accordance with a stereochemically rigid molecule bearing a plane of symmetry containing the molybdenum center, the diazenido fragment, and one dithiocarbamate ligand with a sulfur atom in the equatorial plane and the other one in the apical position.

The mixed-sandwich $[(\eta^5\text{-Cp}')Fe(\eta^6\text{-arene})]^+$ complexes are well-known for their interesting redox behavior.[33,38] For this reason, it was of interest to explore by cyclic voltammetry the electronic influence of the acceptor $[Cp'Fe]^+$ groups through the aryldiazenido linker on the donor $[Mo^{IV}(\eta^2\text{-}S_2CNEt_2)_3]^+$ group. In particular, two complexes, $[(\eta^5\text{-}C_5H_5)Fe(\mu,\eta^6\text{:}\eta^1\text{-}C_6H_5NN)Mo(\eta^2\text{-}S_2CNEt_2)_3]^+PF_6^-$, $\mathbf{5}^+PF_6^-$, and its pentamethylated analogue $[(\eta^5\text{-}C_5Me_5)Fe(\mu,\eta^6\text{:}\eta^1\text{-}C_6H_5NN)Mo(\eta^2\text{-}S_2CNEt_2)_3]^+PF_6^-$, $\mathbf{8}^+PF_6^-$, were chosen for this aim. The voltammograms of both complexes, recorded at room temperature, display three major features:

(i) There is an irreversible cathodic process at −1.89 and −2.12 V, respectively, which one is tempted to assign to the single-electron reduction of the $3d^6$ Fe(II), 18-electron complexes, to the $3d^7$ Fe(I), 19-electron species, at the mixed-sandwich fragment.[33,38] Instead, it turned out that this irreversible wave is attributable to the reduction of the molybdenum center followed by a Mo−S bond cleavage, as found by DFT calculations (vide infra).

(ii) A primary reversible one-electron oxidation wave at $E_{1/2} = 0.41$ V ($\Delta E = 100$ mV) and $E_{1/2} = 0.37$ V ($\Delta E = 110$ mV), respectively, is confidently assigned to a single-electron oxidation of the $4d^2$ Mo(IV), 18-electron complexes, to the $4d^1$ Mo(V), 17-electron species, at the $[Mo^{IV}(\eta^2\text{-}S_2CNEt_2)_3]^+$ fragment (vide infra). According to the ESR investigations of the electro-oxidized complex $[(\eta^1\text{-PhNN})Mo(S_2CNMe_2)_3]^+$, the unpaired electron is essentially located on the molybdenum center.[39] On the other hand, the absence of the $[(\eta^5\text{-}C_5H_5)Fe]^+/[(\eta^5\text{-}C_5Me_5)Fe]^+$ electron-attracting groups is dramatically evidenced by the 380/340 mV cathodic shift observed for the oxidation wave of the parent complex $[(\eta^1\text{-}C_6H_5NN)Mo(\eta^2\text{-}S_2CNEt_2)_3]$, **9** ($E_{1/2} = 0.031$ V, $\Delta E = 102$ mV),[12] thus nicely illustrating the strong electronic cooperativity between the two metal centers. These conclusions are fully consistent with our DFT results (vide infra).

(iii) There is a secondary ill-resolved irreversible oxidation wave at ca. 1.12 and 1.15 V, respectively, similar to that observed for the reported mononuclear complexes $[(\eta^1\text{-ArNN})Mo(\eta^2\text{-}S_2CNMe_2)_3]$.[39] The irreversibility of this oxidation wave is probably due to the fast follow up chemical reaction of the unstable electrode generated trication $[(\eta^5\text{-Cp}')Fe(\mu,\eta^6\text{:}\eta^1\text{-}C_6H_5NN)Mo(\eta^2\text{-}S_2CNEt_2)_3]^{3+}$.

These electrochemical data indicate unambiguously that the electron-withdrawing property of the $[(\eta^5\text{-}C_5H_5)Fe]^+$ group of complex $\mathbf{5}^+PF_6^-$ is stronger than that of $[(\eta^5\text{-}C_5Me_5)Fe]^+$ group of complex $\mathbf{8}^+PF_6^-$ and, therefore, the reduction and oxidation potentials of complex $\mathbf{5}^+PF_6^-$ are more anodic than those of complex $\mathbf{8}^+PF_6^-$.[33] On the other hand, it is clear (and confirmed by DFT calculations; vide infra) that in complexes $\mathbf{5}^+PF_6^-$ and $\mathbf{8}^+PF_6^-$ the character of the LUMO is determined by the cationic mixed sandwich, $[(\eta^5\text{-Cp}')Fe(\eta^6\text{-aryl})]^+$, whereas the nature of the HOMO is centered in the $[Mo(\eta^2\text{-}S_2CNEt_2)_3]^+$ moiety. This is consistent with the electronic spectral data. In fact, the visible spectra of complexes $\mathbf{5}^+PF_6^-$ and $\mathbf{8}^+PF_6^-$ exhibit in $CH_2Cl_2$ a band at 485 nm ($\log \epsilon = 3.76$) and 462 nm ($\log \epsilon = 3.90$), respectively, which can be reasonably attributed to a charge-transfer transition from the $Mo^{IV} \rightarrow Fe^{II}$ through the phenyldiazenido ligand.

**X-ray Crystallographic Studies.** The detailed crystalline and molecular structures of the ionic heterobimetallic complex $\mathbf{7}^+PF_6^-$ and the neutral complex $\mathbf{10}\cdot Et_2O$ were

(38) (a) Astruc, D. In *Electron Transfer and Radical Reactions in Transition-Metal Chemistry*; VCH: New York, 1995; Chapter 2, pp 147−149. (b) Astruc, D. *Chem. Rev.* **1988**, *88*, 1189.

(39) Butler, G.; Chatt, J.; Leigh, G. J.; Pickett, C. J. *J. Chem. Soc., Dalton Trans.* **1979**, 113.

**Table 2.** Selected Bond Lengths (Å) and Bond Angles (deg) for Complexes $7^+PF_6^-$ and **10**·$OEt_2$

| param | $7^+$ | **10**·$OEt_2$ |
|---|---|---|
| | Bond Distances | |
| Mo(1)−N(1) | 1.773(6) | 1.782(4) |
| Mo(1)−S(1) | 2.534(2) | 2.6039(13) |
| Mo(1)−S(2) | 2.530(2) | 2.4865(11) |
| Mo(1)−S(3) | 2.514(2) | 2.5397(12) |
| Mo(1)−S(4) | 2.494(2) | 2.5206(12) |
| Mo(1)−S(5) | 2.575(2) | 2.5283(12) |
| Mo(1)−S(6) | 2.529(2) | 2.5319(12) |
| N(1)−N(2) | 1.276(9) | 1.234(5) |
| N(2)−C[a] | 1.395(10) | 1.428(5) |
| CC[b] | 1.411 | 1.391 |
| Fe(1)−C(26) | 2.140(7) | |
| Fe(1)−C(23) | 2.106(7) | |
| Fe(1)−C(16−20)[c] | 2.046 | |
| Fe(1)−C(21−26)[c] | 2.085 | |
| | Bond Angles | |
| C[a]−N(2)−N(1) | 118.6(7) | 119.7(4) |
| N(2)−N(1)−Mo(1) | 171.5(6) | 170.4(3) |
| N(1)−Mo(1)−S[d] | 170.9(2) | 165.73(11) |
| N(1)−Mo(1)−S[e] | 96.0 | 95.0 |

[a] C′ = C(16) for **10**·$OEt_2$ and C(26) for $7^+$. [b] Average C−C bond length in the phenyl ring, C(16−21) for **10**·$OEt_2$ and C(21−26) for $7^+$. [c] Average Fe−C bond length. [d] S′ = S(1) for **10**·$OEt_2$ and S(5) for $7^+$. [e] Average bond angle made by the apical nitrogen, the molybdenum, and the equatorial sulfurs atoms, S(2−6) for **10**·$OEt_2$ and S(1−4,6) for $7^+$.

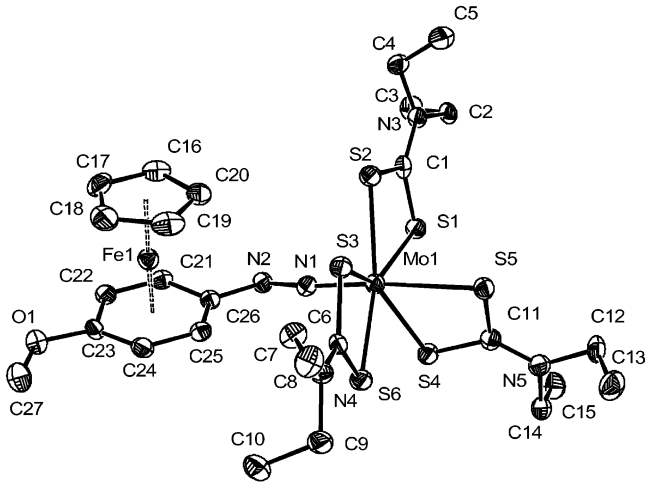


**Figure 2.** Molecular structure and atom numbering scheme for $7^+$. Hydrogen atoms and the $PF_6^-$ counterion have been omitted for clarity. Displacement ellipsoids are shown at the 30% probability level.

unambiguously determined by X-ray diffraction studies as outlined in the Experimental Section and Table 1. Key bond lengths and angles are listed in Table 2. Drawings of the cationic organometallic entity $7^+$ and the neutral species **10**, along with the atom-numbering scheme, are depicted in Figures 2 and 3, respectively. Likewise, for the sake of comparison, Table 3 contains the relevant bond lengths and bond angles of the heterobinuclear aryldiazenido cores of $7^+$ and those of Cr−W, $Ru^+$−W, and $Fe^+$−W described by Hidai et al.[8] This table also includes the metrical parameters of three classic aryldiazenido molybdenum cores of general formula $[(\eta^1\text{-}RC_6H_4NN)Mo(S_2CNMe_2)_3]$, R = H and m-$NO_2$,[40] and **10**·$Et_2O$ that do not contain the electron-attracting $CpFe^+$ fragment.

Complex $7^+PF_6^-$ crystallizes in the triclinic space group $P\bar{1}$ with 2 crystallographically inequivalent molecules/asymmetric unit, the difference between the two molecules being essentially due to very slight variations in the conformation of the ethyl groups. The cationic entity $7^+$ consists of an organometallic moiety $[(\eta^5\text{-Cp})Fe]^+$ and an inorganic fragment $[Mo(\eta^2\text{-}S_2CNEt_2)_3]^+$, both connected through the $\pi$-conjugated aryldiazenido bridge, $[p\text{-}MeOC_6H_4-N{=}N]^-$, in $\eta^6$ and $\eta^1$ mode. The $Mo^{IV}$ center possesses the seven-coordinate pentagonal bipyramidal structure, with two $[Et_2NCS_2]^-$ ligands in the equatorial plane in an $\eta^2$ mode and the third spanning an axial and an equatorial position. The aryldiazenido ligand whose oxidation state is −1[4] occupies the remaining axial position through the terminal Nα atom in a $\eta^1$ fashion. The aryl group is hexahapto coordinated to the $[(\eta^5\text{-Cp})Fe]^+$ moiety. In the mixed sandwich fragment, the iron atom is coordinated to the cyclopentadienyl ring at a ring centroid−iron distance of 1.664 Å and to the aryl ring at a ring centroid−iron distance of 1.536 Å. A careful examination of Table 3 reveals some interesting features provoked by the strong electron-withdrawing $CpFe^+$ moiety on the aryldiazenido ligand. In fact, one of the most remarkable deviation observed in the molecular parameters of this complex correspond to the Fe−$C_{ipso}$ bond length, 2.140(7) Å, which is ca. 0.065 Å longer than the mean of the other Fe−C ($C_6$ ring) bond lengths. Likewise, the $C_{ipso}$−N bond length, 1.395(10) Å, is ca. 0.042 Å shorter than the mean reported for a C−N single bond.[41] Such features had also been observed by Hidai et al. in related heterobinuclear aryldiazenido complexes[8,9] although the elongation and shortening observed in the M−$C_{ipso}$ and $C_{ipso}$−N bonds, respectively, were much more dramatic than that observed in $7^+$ (see Table 3). These observations were rationalized by Hidai et al. assuming that the aryldiazenido linker receives an important contribution of the zwitterionic resonance structure as a consequence of the presence of both the electron-rich $W^{II}(5d^4)$ center and the $(CO)_3Cr$, $[(\eta^5\text{-Cp})Fe]^+$, or $[(\eta^5\text{-Cp})Ru]^+$ electron-withdrawing groups.[7,8] These observations lead us also to attribute to the species $7^+$ a partial positive charge on the molybdenum center and, consequently, a cyclohexadienyl-like character of the arene ring with a partial negative charge and a dihedral folding angle of 6.0(8)° (Chart 1). These findings are in accord with previous structural data[42] and theoretical work[43] and more recently in several diiron and triiron organometallic hydrazones.[11] In the case of complex $7^+$, the presence of both a $Mo^{IV}(4d^2)$ center and the electron-withdrawing $[(\eta^5\text{-Cp})Fe]^+$ group must stabilize the charge-separated resonance structure

(40) Butler, G.; Chatt, J.; Leigh, G. J.; Smith, A. R. P.; Williams, G. A. *Inorg. Chim. Acta* **1978**, *28*, L165.
(41) Orpen, A. G.; Bramer, L.; Allen, F. H.; Kennard, D.; Watson, D. G.; Taylor, R. *J. Chem. Soc., Dalton Trans.* **1989**, *S1*.
(42) (a) Saillard, J.-Y.; Grandjean, D.; Le Maux, P.; Jaouen, G. *Nouv. J. Chim.* **1981**, *5*, 153. (b) Hunter, A. D.; Shilliday, L.; Furey, W. S.; Zaworotko, M. J. *Organometallics* **1992**, *11*, 1550. (c) Lambert, C.; Gaschler, W.; Matschiner, R.; Wortmann, R. *J. Organomet. Chem.* **1999**, *592*, 109. (d) Djukic, J.-P.; Rose-Munch, F.; Rose, E.; Vaissermann, J. *Eur. J. Inorg. Chem.* **2000**, *1295*. (e) Moriuchi, A.; Uchida, K.; Inagaki, A.; Akita, M. *Organometallics* **2005**, *24*, 6382.
(43) Ruiz, J.; Ogliaro, F.; Saillard, J.-Y.; Halet, J.-F.; Varret, F.; Astruc, D. *J. Am. Chem. Soc.* **1998**, *120*, 11693.

**Chart 1**

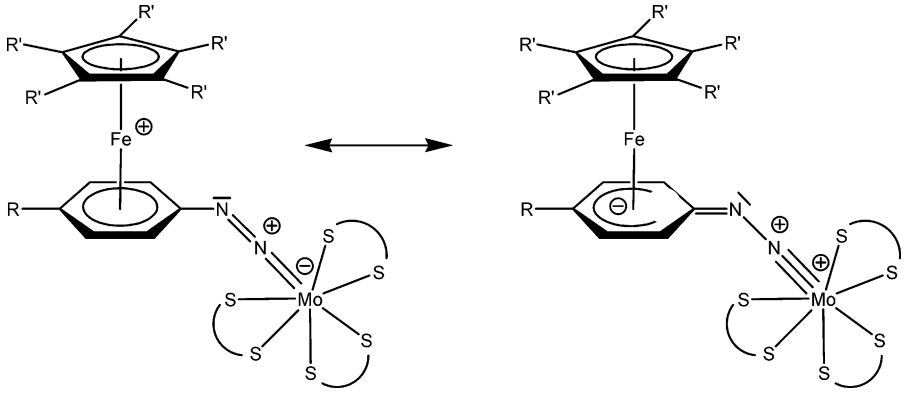

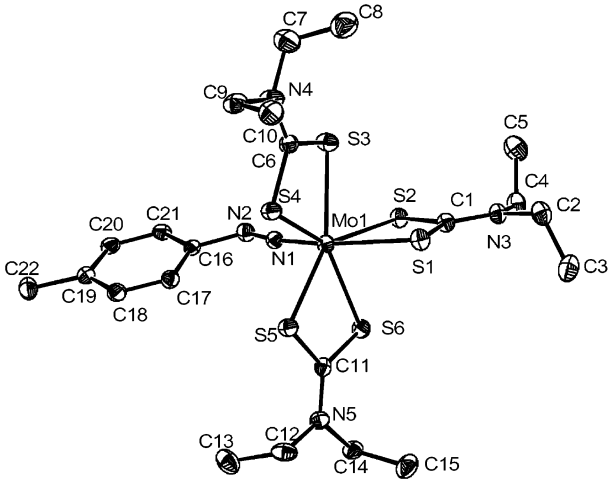

**Figure 3.** Molecular structure and atom numbering scheme for **10**. Hydrogen atoms and the solvent molecule have been omitted for clarity. Displacement ellipsoids are shown at the 30% probability level.

of the aryldiazenido ligand. In classic aryldiazenido molybdenum complexes, which do not contain electron-withdrawing moieties, these structural changes are obviously not observed and the $C_{ipso}$−N bond lengths lie in the normal range 1.41−1.43 Å (see Table 3). On the other hand, the N−N bond length of **7**$^+$, 1.276(9) Å, compares well with those reported by Hidai et al.[8] (Table 3), but they are longer than those measured in the classic (aryldiazenido)molybdenum complexes, whose N═N bond lengths conserve the double-bond character.[2,40] Finally, the Mo═N bond length determined in complex **7**$^+$, 1.773(6) Å, seems to be unexceptional for a MoN double bond[2] and too long for a triple bond. This bond length cannot be compared with those observed in the complexes reported by Hidai et al.[8] due to the different oxidation states of the involved metal centers, $Mo^{IV}$ and $W^{II}$, giving rise to different external electronic configurations, $4d^2$ and $5d^4$, respectively, and different ionic radii.

Complex **10**·$Et_2O$, of formula [($\eta^1$-*p*-$MeC_6H_4N$═N)Mo($\eta^2$-$S_2CNEt_2)_3$]·$Et_2O$, also crystallizes in the triclinic space group $P\bar{1}$ as a diethyl ether solvate, with one independent molecule/asymmetric unit (see Experimental Section and Table 1). This complex is analogue to the classic complexes reported by Chatt et al.[40] and does not deserve further discussion (see Table 3 for key bond lengths and angles).

**Theoretical Investigations.** To get a better understanding of the properties of the title compound and on the iron−molybdenum communication along the aryldiazenido bridge, we have carried out DFT calculations on a simplified model of **7**$^+$ in which the ethyl groups of the dithiocarbamato ligands are replaced by hydrogen atoms. The monooxidized and monoreduced states have been also computed. These model complexes are labeled **7′**$^+$, **7′**$^{2+}$, and **7′**, respectively. The mononuclear species **10** has been modelized in the same manner, and its monooxidized and monoreduced states were also computed. These models are labeled **10′**, **10′**$^+$, and **10′**$^-$, respectively. Computational details are given in the Experimental Section. Major optimized bond distances and angles and other selected computed data are given in Table 4. The MO diagrams of **10′** and **7′**$^+$ are shown in Figure 4.

The optimized geometries of **7′**$^+$ and **10′** are in good agreement with the X-ray structures of **7**$^+$ and **10**. As usually found with this type of calculations, the computed metal−ligand distances are slightly longer than the experimental ones. The opposite trend is observed for the N−N distances. The HOMO of **10′** lies somewhat isolated 0.78 eV above the HOMO-1 (left-hand side of Figure 4). It can be described as a Mo d-type lone-pair (48%) mixed in a bonding way with the $\pi$*(NN) orbital (20%). This orbital can be considered as containing the two d electrons of the $Mo^{IV}$ center, since all the other occupied MOs have minor metal participation. The HOMO-1 can be associated with the N(2) lone pair, mixed in an antibonding way with the $\pi$-bonding Mo−N electron pair. It has N(1), N(2), and Mo participations of 14%, 17%, and 25%, respectively. The lowest unoccupied orbitals are Mo−S antibonding. The LUMO and LUMO+1 have similar localization on Mo (55% and 57%, respectively) and on S (40% and 43%, respectively). Complexing the phenyl ring by a $CpFe^+$ moiety merely perturbs these features, as it can be seen on the MO diagram of **7′**$^+$ (right-hand side of Figure 4). The only important change is the inclusion of five Fe(II) d-type levels in the diagram. The occupied Fe "$t_{2g}$" levels are associated with the HOMO-4, HOMO-5, and HOMO-7. The two other Fe d-type AOs (the so-called "$e_g$*" set) correspond to the LUMO and LUMO+1. They are largely Fe−Cp antibonding, with similar localization on Fe (53% and 62%, respectively) and on Cp (19% and 26%, respectively). The LUMO has some Mo participa-

**Table 3.** Comparison of Selected Bond Lengths (Å) and Bond Angles (deg) of Heterobimetallic Aryldiazenido Cores and Mononuclear Related Complexes

| compd | bond lengths (Å)/bond angles (deg) | | | | | | ref |
|---|---|---|---|---|---|---|---|
| | M−$C_{ipso}$ | $C_{ipso}$−N | NN | N−M | M−NN | NN−C | |
| [{$(CO)_3$Cr($\mu$-$\eta^6$:$\eta^1$-*p*-$C_6H_4CO_2$Me)N═N}W(NCS)(dppe)$_2$][a] | 2.431(5) | 1.366(6) | 1.314(5) | 1.784(4) | 164.9(3) | 120.0(4) | 8 |
| [{$(CO)_3$Cr($\mu$-$\eta^6$:$\eta^1$-*p*-$C_6H_4CO_2$Me)N═N}WF(dppe)$_2$][a] | 2.50(1) | 1.30(2) | 1.33(2) | 1.80(1) | 161(1) | 117(1) | 8 |
| [{CpRu($\mu$-$\eta^6$:$\eta^1$-$C_6H_5$)N═N}W(NCS)(dppe)$_2$]$^+$ [a] | 2.39(2) | 1.40(2) | 1.28(1) | 1.75(1) | 166(1) | 122(11) | 8 |
| [{CpFe($\mu$-$\eta^6$:$\eta^1$*p*-$C_6H_4$Me)N═N}WF(dppe)$_2$][a] | 2.24(1) | 1.35(1) | 1.32(1) | 1.778(8) | 164.0(7) | 120.6(8) | 8 |
| [{CpFe($\mu$-$\eta^6$:$\eta^1$*p*-$C_6H_4$Me)N═N}Mo($Et_2$-dtc)$_3$]$^+$ [b] (**7**$^+$) | 2.140(7) | 1.395(10) | 1.276(9) | 1.773(6) | 171.5(6) | 118.6(7) | this work |
| [{$(C_6H_5)$N═N}Mo($Me_2$-dtc)$_3$][b] | | 1.417(7) | 1.233(6) | 1.781(4) | 171.5(4) | 120.5(5) | 40 |
| [{(*m*-$C_6H_4NO_2$)N═N}Mo($Me_2$-dtc)$_3$][b] | | 1.410(10) | 1.262(9) | 1.770(6) | 170.6(6) | 117.9(7) | 40 |
| **[{(*p*-$C_6H_4$Me)N═N}Mo($Et_2$-dtc)$_3$][b] (10)** | | 1.428(5) | 1.234(5) | 1.782(4) | 170.4(3) | 118.6(7) | this work |

[a] dppe = bis(diphenylphosphino)ethane. [b] dtc = dithiocarbamate.

**Table 4.** Major Computed Data for **7′**$^{2+/+/0}$ and **10′**$^{+/0/-}$

| param | **7**$^{+2}$ | **7**$^+$ | **7** | **10**$^+$ | **10** | **10**$^-$ |
|---|---|---|---|---|---|---|
| first ionization energy (eV) | | 8.97 | | | 5.96 | |
| electronic affinity (eV) | | 4.23 | | | 1.63 | |
| HOMO−LUMO gap (eV) | | 1.78 | | | 1.68 | |
| dipole moment (D) | 23.33 | 14.70 | 7.77 | 5.70 | 2.14 | 5.59 |
| bond dists (Å) | | | | | | |
| Mo(1)−N(1) | 1.906 | 1.833 | 1.817 | 1.909 | 1.847 | 1.827 |
| Mo(1)−S(1) | 2.580 | 2.586 | 2.581 | 2.570 | 2.665 | 2.731 |
| Mo(1)−S(2) | 2.550 | 2.611 | 2.918 | 2.558 | 2.564 | 2.551 |
| Mo(1)−S(3) | 2.576 | 2.614 | 2.839 | 2.578 | 2.598 | 2.636 |
| Mo(1)−S(4) | 2.565 | 2.553 | 2.535 | 2.588 | 2.608 | 2.585 |
| Mo(1)−S(5) | 2.560 | 2.634 | 2.676 | 2.602 | 2.611 | 3.857 |
| Mo(1)−S(6) | 2.593 | 2.613 | 2.657 | 2.567 | 2.604 | 2.561 |
| N(1)−N(2) | 1.217 | 1.244 | 1.268 | 1.207 | 1.222 | 1.244 |
| N(2)−Ca | 1.418 | 1.390 | 1.371 | 1.406 | 1.413 | 1.404 |
| C−Cb | 1.427 | 1.428 | 1.430 | 1.409 | 1.408 | 1.410 |
| Fe(1)−C(26) | 2.109 | 2.184 | 2.261 | | | |
| Fe(1)−C(23) | 2.210 | 2.149 | 2.105 | | | |
| Fe(1)−C(16−20)[c] | 2.094 | 2.092 | 2.103 | | | |
| Fe(1)−C(21−26)[c] | | 2.124 | 2.121 | | | |
| bond angles (deg) | | | | | | |
| Ca−N(2)−N(1) | 123.2 | 121.0 | 118.9 | 125.3 | 123.2 | 121.3 |
| N(2)−N(1)−Mo(1) | 171.2 | 171.8 | 173.4 | 172.0 | 172.0 | 174.3 |
| N(1)−Mo(1)−Sd | 167.6 | 169.5 | 169.2 | 169.4 | 168.2 | 169.0 |
| N(1)−Mo(1)−Se | 95.9 | 96.4 | 97.3 | 94.4 | 95.3 | 97.9 |

tion (12%). The Mo−S antibonding levels lie just above the LUMO+1.

Oxidizing **10′** and **7′**$^+$ consists in removing one electron from similar HOMOs. Since this orbital is NN antibonding and Mo−N bonding (Figure 4), N−N shortening and Mo−N lengthening result (Table 4). This oxidation can be described as a $Mo^{IV}$ to $Mo^V$ oxidation change, as exemplified by the spin density plots of **10′**$^+$ and **7′**$^{2+}$ shown in Figure 5. Interestingly, the ionization potentials of **10′** and **7′**$^+$ are different (Table 4). Due to its cationic charge, the oxidation of **7′**$^+$ requires more energy than that of neutral **10′**. This result is in full agreement with the electrochemical experiments discussed above.

At first sight, the monoelectronic reductions of **10′** and **7′**$^+$ might be expected to be different because of the different nature of their LUMO's. Indeed, reducing **7′**$^+$ may lead to predict the formation of a CpFe(I)($\eta^6$-aryl) entity (vide supra). Calculations actually show that this is not the case. Mo−S decoordination is found for both **10′**$^-$ and **7′**. In the case of **10′**$^-$, the Mo−S(5) distance (3.86 Å) is definitely nonbonding. In the case of **7′**, Mo−S(2) (2.92 Å) and Mo−S(3) (2.84 Å) are also nonbonding or weakly bonding. Also one cannot ascertain that we found the structure of lowest energy for **10′**$^-$ and **7′**, our calculations show clearly that reduction of **10′** or **7′**$^+$ leads in both cases to partial decoordination of the dithiocarbamato ligands with the formation of a formally $Mo^{III}$ metal center as exemplified by the spin density plots of **10′**$^-$ and **7′** shown in Figure 5. Thus, in the case of **7′**, sulfur decoordination provides more stabilization than creating a Fe(I) 19-electron center. It should be noted, however, that, in this compound, small but significant spin density is computed on Fe (0.11, vs 0.53 on Mo), indicative of the electron-withdrawing effect of the $CpFe^+$ moiety. Similarly to their ionization potentials, the electronic affinities of **10′** and **7′**$^+$ are significantly different (Table 4), mainly because of their different electric charges. Thus, it is easier to reduce **7′**$^+$ than **10′**. This result is consistent with the electrochemical experiments discussed above.

TD-DFT calculations have also been carried out on **7′** in vacuum (see computational details) to ascertain the nature of the more intense visible bands of Figure 1. The computed wavelengths are much larger than their experimental counterparts. This may be partly due to the ligand simplification in the computed model but more likely because solvent effects were not considered in the calculations. Nevertheless, they are consistent with the two-band shape of the spectrum shown in Figure 1. The less energetic computed transition (736 nm) can be assigned to the band observed at ~470 nm

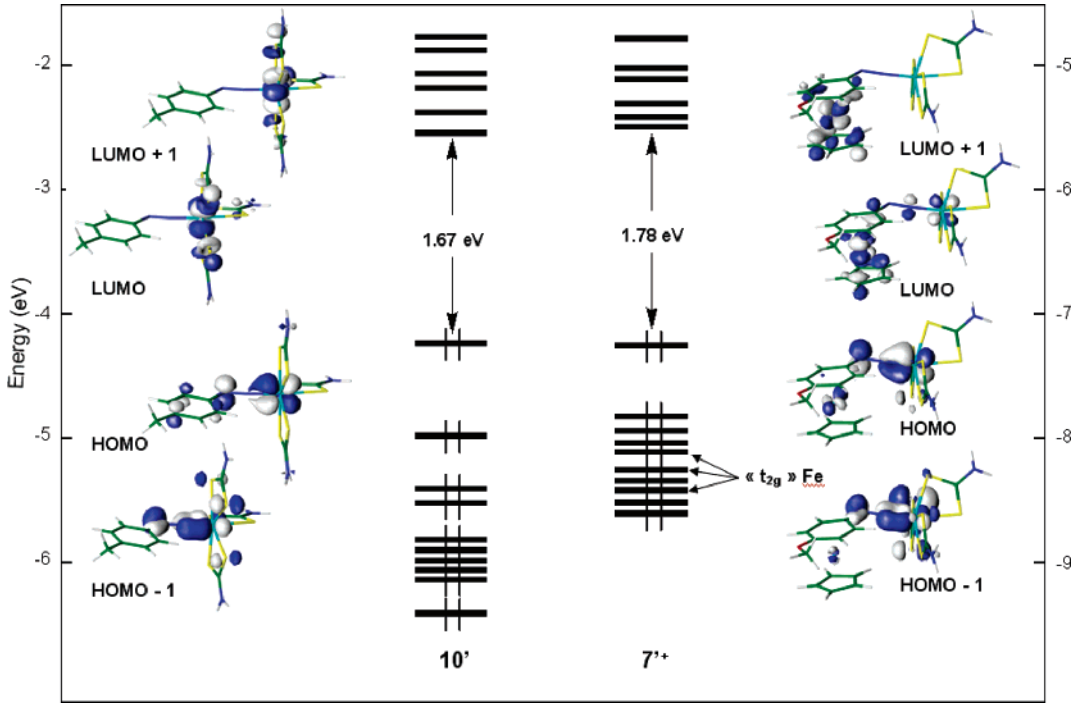


**Figure 4.** Molecular Orbital diagrams of $\mathbf{7'}^{+}$ and $\mathbf{10'}$.

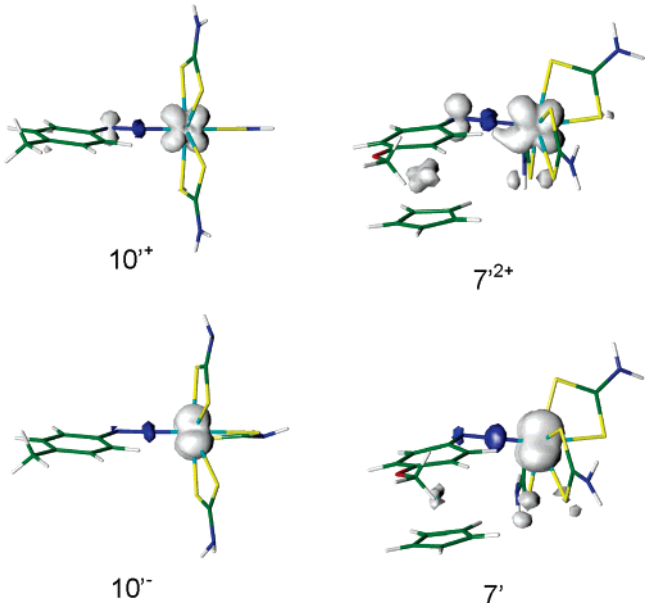


**Figure 5.** Plots of the computed spin densities of $\mathbf{10'}^{+}$, $\mathbf{7'}^{2+}$, $\mathbf{10'}^{-}$, and $\mathbf{7'}$.

(Figure 1). It corresponds to transitions from the HOMO to the LUMO and LUMO+1, confirming its Mo to Fe charge-transfer nature. A nearby computed transition at 669 nm with a 60% weaker oscillator strength corresponds to mixed ligand/Mo charge transfer to Fe. This transition likely contributes also somewhat to the band observed at ~470 nm. The next strong excitation is computed at 491 nm and can be assigned to the band observed at ~380 nm (Figure 1). It corresponds to transitions from the HOMO to two antibonding ligand-based MOs which are of dithiocarbamato and aryldiazenido nature, respectively, confirming the Mo to ligand charge-transfer nature of this band (vide supra). Another transition which should contribute as a minor component to this observed band is computed at 467 nm and corresponds to mixed ligand/Mo charge transfer to ligand.

## Conclusions

As a result of this study, we have succeeded in the synthesis of representative members of a new family of covalently bonded charge-transfer molecular hybrids of general formula $[(\eta^5\text{-Cp})\text{Fe}(\mu,\eta^6{:}\eta^1\text{-}p\text{-RC}_6\text{H}_4\text{NN})\text{Mo}(\eta^2\text{-S}_2\text{CNEt}_2)_3]^+\text{PF}_6^-$, $\mathbf{5}^+\text{PF}_6^- - \mathbf{7}^+\text{PF}_6^-$, and $[(\eta^5\text{-C}_5\text{Me}_5)\text{Fe}(\mu,\eta^6{:}\eta^1\text{-C}_6\text{H}_5\text{NN})\text{Mo}(\eta^2\text{-S}_2\text{CNEt}_2)_3]^+\text{PF}_6^-$, $\mathbf{8}^+\text{PF}_6^-$. These hybrid complexes consist of organometallic and inorganic fragments, $[(\eta^5\text{-Cp})\text{Fe}]^+$ and $[\text{Mo}(\eta^2\text{-S}_2\text{CNEt}_2)_3]^+$, respectively, which are connected one other by an aryldiazenido spacer, $[\text{RC}_6\text{H}_4\text{N}{=}\text{N}]^-$, in a $\mu,\eta^6{:}\eta^1$ mode through the $\pi$-system of the aryl group and the $\sigma-\pi$ orbitals of the diazenido group. Moreover, electronic spectra and electrochemical and structural data in conjunction with theoretical investigations clearly indicate the existence of a charge-transfer transition from the inorganic donor to the organometallic acceptor fragments through the aryldiazenido spacer. The readiness with which the organometallic arylhydrazines form these new molecular architectures with dioxomolybdenum complexes represents an alternative strategy to those described by Hidai et al.[8] for the preparation of new charge-transfer hybrids and could be extended to other transition metal complexes containing oxometal functionalities, e.g., Re=O and W=O. Along this line, we are currently extending this new strategy to Lindqvist hexamolybdate species to prepare new organometallic−inorganic charge-transfer hybrids.

**Acknowledgment.** Thanks are expressed to Drs. S. Sinbandhit, P. Jehan, and P. Guénot (CRMPO, Rennes, France) for skillful assistance in recording high-field NMR

and high-resolution mass spectrometry. Financial support from the Fondo Nacional de Desarrollo Científico y Tecnológico, FONDECYT-Chile, Grant Nos. 1980433 and 1060490, is gratefully acknowledged. Computing facilities were provided by the PCIO Center at the University of Rennes 1 and the IDRIS-CNRS Center at Orsay, France.

**Supporting Information Available:** Crystallographic files in CIF format for the two reported X-ray crystal structures. This material is available free of charge via the Internet at http://pubs.acs.org.

IC0613098